Supporting Information

Boosting one-step conversion of cyclohexane to adipic acid by NO_2 and VPO composite catalysts

Jian Jian [a], Kuiyi You [a,b,*], Xuezhi Duan [c], Hongxu Gao [a] , Qing Luo [a], Renjie Deng [a] , Pingle Liu [a,b], Qiuhong Ai [a,b] and He'an Luo [a,b,*]

[a] *School of Chemical Engineering, Xiangtan University, Xiangtan 411105, P.R., China.*

[b] *National & Local United Engineering Research Center for Chemical Process Simulation and Intensification, Xiangtan University, Xiangtan 411105, P. R., China*

[c] *State Key Laboratory of Chemical Engineering, East China University of Science and Technology, Shanghai 200237, P. R. China*

*Corresponding authors:
E-mail: youkuiyi@126.com (K. You); hluo@xtu.edu.cn (H. Luo)

CONTENTS:

23

1. Experimental Section:

1.1 Reagents and instrument

Cyclohexane (AR) was purchased from Shanghai Chemical Co. Ltd., China. NO_2 (purity ＞99.9%) was purchased from Beijing chemical Co. Ltd., China. Except where specified, all chemicals were of analytical grade and used as purchased. Gas chromatography (GC) was performed on Shimadzu GC-2010 Plus equipped with an RTX-5 (30m×0.25mm×0.25um) column. Gas chromatography-Mass spectrometry (GC-MS) was run on a Shimadzu GCMS-QP2010 Plus. High performance liquid chromatograph (HPLC) was performed on an Agilent 1260 with 15:75:10 (V/V) of CH_3OH:H_2O:KH_2PO_4 as mobile phase, detected at 210nm of wavelength and 1.0 ml/min of flow.

1.2 The preparation and characterization of catalyst

A series of VPO composite catalysts were prepared according to the following procedure. Typically, 4.75 g of $Ni(Ac)_2 \cdot 4H_2O$, 2.275 g V_2O_5 and 1.275 g γ-Al_2O_3 was suspended in a 1:1 (v/v) mixture of isobutyl alcohol and benzyl alcohol in a 100 ml three-necked, round-bottomed flask reactor equipped with a reflux condenser and a magnetic stirrer. The suspension was stirred under reflux for 3 h at 110 ^oC. Subsequently, 85% H_3PO_4 was added dropwise to reach a P/V atomic ratio of 1.2/1.0. After

refluxing for another 3 h, the suspension was filtered under reduced pressure and the resulting solid was dried in air at 120 ^{o}C for 10 h. Finally, the samples were heated from room temperature to 500 ^{o}C at a rate of 2 ^{o}C min^{-1} in dry air and kept at this temperature for 5 h. All of these samples were activated in situ before characterization and performance evaluation.

The X-ray diffraction (XRD) analysis of VPO composites was performed in a Rigaku D/max2550 18KW Rotating Anode X-ray Diffractometer with monochromatic Cu Kα radiation (λ = 1.5418 Å) radiation at voltage and current of 40 kV and 300 mA. The morphology of samples was recorded with high-resolution transmission electron microscopy (HRTEM) on JEM-2100F with an accelerating voltage of 200kV. ICP-OES (Optima 3000XL, Perkin-Elmer) using a microwave pressure digestion (MDS 200; CEM) with hydrofluoric acid and aquaregia at 9 bar was used to analyze the chemical composition of catalysts. All the samples were analyzed twice and the results presented here are the average values. The X-ray photoelectron spectroscopy (XPS) measurement were performed on a K-Alpha 1063 spectrometer (ThermoFisher Scientific, U.K.) with Al Kα radiation at settings of 12 KV and 6 mA. Binding energies (BEs) for each element were referred to the C1s signal (284.8 eV). The fitting of the XPS peaks was done by least-squares using Gaussian-Lorentzian peak shapes. The UV-vis spectra

of the catalysts were obtained by UV-2550 spectrophotometry. The spectrum was recorded in range of 200-800 nm using barium sulphate as the reflectance standard. Fourier transform infrared (FT-IR) spectra were collected on a Nicolet 380 spectrometer. The spectra of the samples were acquired in the wave number range of 360-4000 cm^{-1}. The temperature programmed reduction with hydrogen (H_2-TPR) were carried out using a Quantachrome Instruments CHEMBET 3000. The sample (100 mg) was reduced with a 5% H_2/Ar mixture (30 $ml \cdot min^{-1}$) by heating room temperature to 1273 K at a rate of 10 $K \cdot min^{-1}$.

1.3 Typical experimental procedure

The catalytic oxidation reaction was performed in a 150 ml sealed autoclave with magnetic stirrer and temperature-controlling device. Firstly, the mixtures of cyclohexane and nitrogen dioxide were prepared by pouring the liquid nitrogen dioxide into a known weight of chilled cyclohexane and determining the total weight, nitrogen dioxide was completely soluble in cyclohexane. And then the cold nitrogen dioxide-cyclohexane solution was poured into the sealed autoclave. The sealed autoclave was immersed in an oil bath maintained at a preselected temperature. Typically, 5.04 g (0.06 mol) cyclohexane and 13.80 g (0.30mol) liquid NO_2 were added into the autoclave. The reaction mixture was stirred at 80 ^oC for 24 h. After cooling to room temperature, the

resulting mixture was divided into three phases. The liquid phase collected products were quantified by internal standard methods (chlorobenzene was used as internal standard sample) from GC with FID detector. The solid phase products were separated by filtration, washed with methylene dichloride, dried at 60 ^{o}C in vacuum for 24 h, finally dissolved in methanol and quantified by HPLC external standard calibration curve method. The unsolvable catalyst was separated and washed with distilled water several times, dried at 110 ^{o}C and reused for the next run. The components of gas phase were analyzed by GC with TCD detector. The identifications of all products were done by GC-MS and LC-MS. The white crystal separated from solid phase is characterized by comparison of its spectral and physical data with the authentic sample of adipic acid. The conversion of cyclohexane and selectivity of adipic acid and nitrocyclohexane were calculated by the following formula:

$$\text{Conversion of cyclohexane (\%)} = \frac{\left[\begin{array}{c}\text{the amount (mol) of}\\ \text{starting cyclohexane}\end{array}\right] - \left[\begin{array}{c}\text{the amount (mol) of}\\ \text{cyclohexane recovered}\end{array}\right]}{\text{the amount (mol) of starting cyclohexane}} \times 100\%$$

$$\text{Selectivity of adipic acid (\%)} = \frac{\text{the amount (mol) of adipic acid}}{\left[\begin{array}{c}\text{the amount (mol) of}\\ \text{starting cyclohexane}\end{array}\right] - \left[\begin{array}{c}\text{the amount (mol) of}\\ \text{cyclohexane recovered}\end{array}\right]} \times 100\%$$

$$\text{Selectivity of nitrocyclohexane (\%)} = \frac{\text{the amount (mol) of nitrocyclohexane}}{\left[\begin{array}{c}\text{the amount (mol) of}\\ \text{starting cyclohexane}\end{array}\right] - \left[\begin{array}{c}\text{the amount (mol) of}\\ \text{cyclohexane recovered}\end{array}\right]} \times 100\%$$

2. Figures and Tables Captions:

Figure S1 Effects of reaction temperature on the oxidation reaction of cyclohexane with NO_2. Reaction conditions: the molar ratio of cyclohexane to NO_2 is 0.2:1, reaction time is 24 h.

Figure S2 Effects of reaction time on the oxidation reaction of cyclohexane with NO_2. Reaction conditions: the molar ratio of cyclohexane to NO_2 is 0.2:1; reaction temperature is 80 ºC.

Figure S3 The XRD patterns of typical VPO composite catalysts.

Figure S4 The FT-IR spectra of typical VPO composite catalysts.

Figure S5 The UV-vis DRS spectra of typical VPO composite catalysts

Figure S6 The H_2-TPR profiles of typical VPO composite catalysts

Figure S7 The TEM images of typical VPO catalysts: (a) VPO precursor, (b) VPO, (c) Al-VPO, (d) Ni-Al-VPO

Table S1 Effects of molar ratio of cyclohexane to NO_2 on the oxidation reaction.

Table S2 Composition of the elements in the several VPO composite catalysts.

Table S3 Data of Ni-Al-VPO catalyst recycling and leaching

3. Figures and Tables

3.1 Effects of reaction temperature on the oxidation reaction of cyclohexane with NO_2

Effects of reaction temperature on the conversion of cyclohexane and the selectivity of adipic acid in the oxidation reaction were examined, and the results (see **Figure S1**) indicated that the reaction temperature was a significant factor to conversion and selectivity from the catalytic oxidation of cyclohexane and NO_2. And a range of favorable reaction temperature should be about 80 ºC from the points of selectivity of adipic acid.

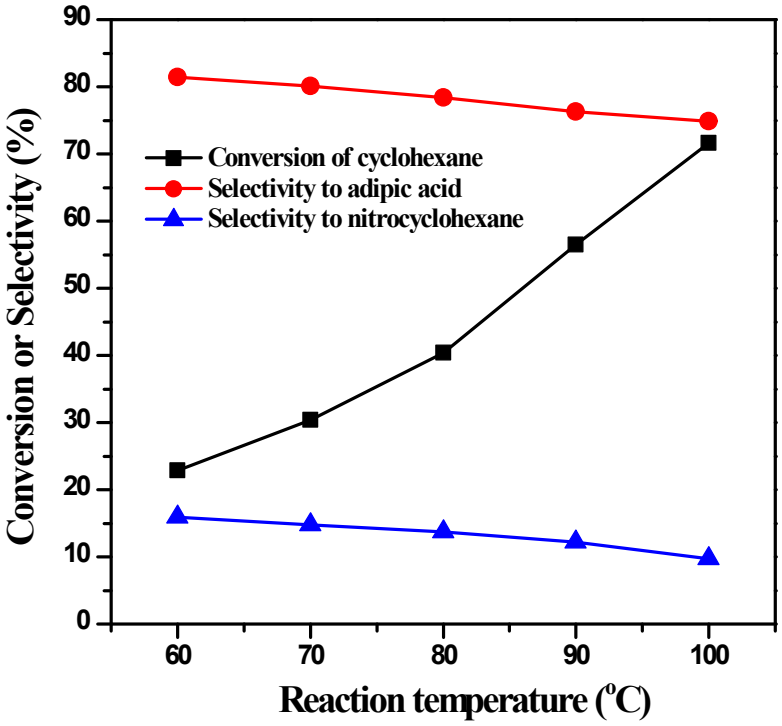

Figure S1

3.2 Effects of reaction time on the oxidation reaction of cyclohexane with NO_2

The Effects of reaction time on the oxidation reaction were depicted in **Figure S2**. The results showed that the reaction time was also an important factor to the selectivities of adipic acid in the oxidation reaction of cyclohexane with NO_2. From the points of selectivity of adipic acid, obviously, a favorable reaction time should be 24 h at 80 ºC.

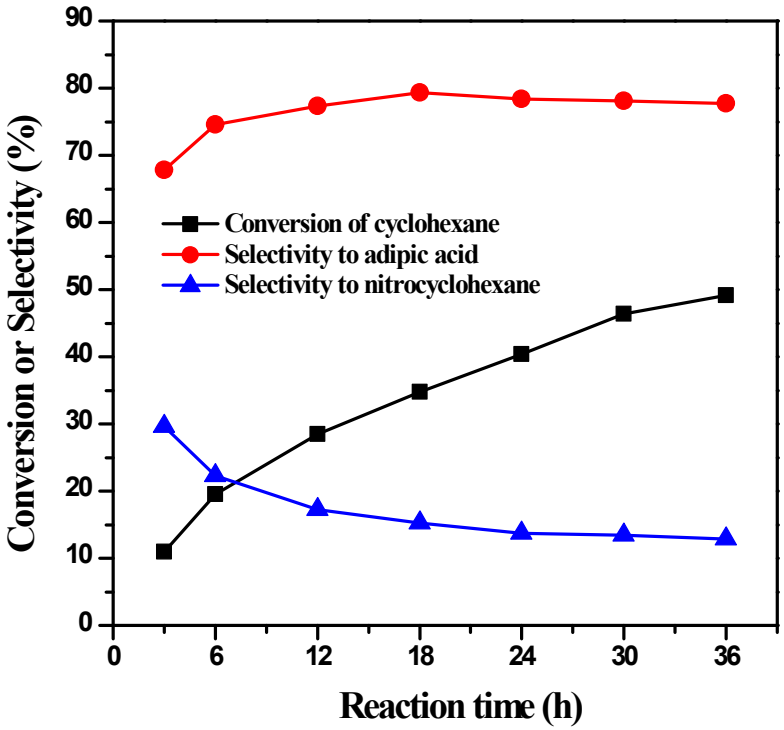

Figure S2

3.3 X-ray diffraction studies

The XRD patterns of typical VPO composite catalysts were shown in **Figure S3**. The reduced VPO shows the characteristic reflections of vanadyl hydrogen phosphate hemihydrate $VOHPO_4 \bullet 0.5H_2O$ (JCPDS: 37-0269), with the main intensity peaks at 2θ values of 15.5°, 19.5°, 24.1°, 27.1° and 30.4°. This indicates that vanadium in the VPO precursor is V^{4+} state. The XRD patterns of activated VPO and Al promoted VPO (Al-VPO) catalysts are very similar, both shows high intensity peaks at 2θ values of 11.9°, 18.6°, 23.9°, 28.7°, 31.2°, 41.1° and 46.4°, characteristic of the $VOPO_4 \bullet 2H_2O$ phase (JCPDS: 36-1472), and also low intensity peaks at 2θ values 25.6°, 26.2°, 29.1° and 30.0°, characteristic of the *β*-$VOPO_4$ phase (JCPDS: 24-0948), the intensity peaks at 2θ values at 2θ values of 18.5°, 21.6° and 28.3°, characteristic of the $(VO)_2P_2O_7$ phase (JCPDS: 41-0697). This suggests that vanadium in the sole VPO catalyst and Al-VPO catalyst samples is predominantly in the V^{5+} state with a small amount of V^{4+} species, which was in accordance with the XPS measurement (**Figure 2**). In addition, the X-ray lines of Al-VPO is broadened and diminished as compared to the sole VPO. This shows that Al component does not change the structure of the active components of VPO, but reduces the crystallinity and forms a smaller size of crystallites. This may be the reason why the BET surface areas of Al-VPO gave

higher value, 19.7 m^2 g^{-1} compare to 14.1 m^2 g^{-1} for VPO. Therefore, Al-VPO catalyst has higher catalytic activity compare to VPO due to higher surface area of vanadium phosphorus oxide having a number of active sites per unit mass of catalyst. In the case of Al-VPO composite catalyst combined nickel (Ni-Al-VPO), the XRD patterns become more complicated. The intensity of characteristic peaks of $(VO)_2P_2O_7$ phase is greater than the characteristic peaks of β-$VOPO_4$ phase, which implies that doped Ni component results in the increase of V^{4+} and the decrease of V^{5+}. Besides, the $Ni_2P_2O_7$ phase (JCPDS: 39-0710) (with the representative peaks at 2θ values of 17.5°, 30.4°and 35.4°) was observed in the Ni-Al-VPO sample.

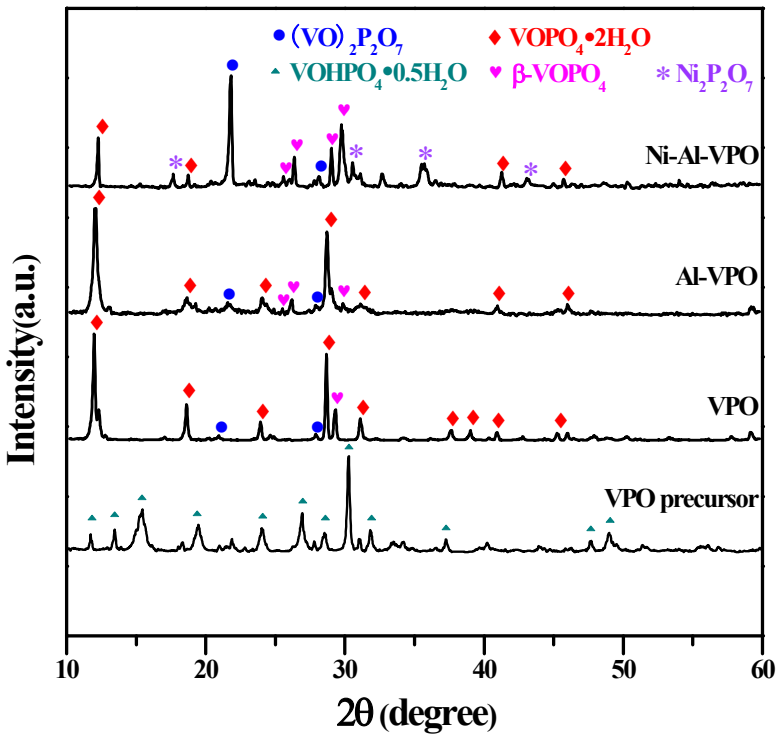

Figure S3

3.4 FT-IR spectra studies

The FT-IR spectra of typical VPO composite catalysts were depicted in **Figure S4**. All of the catalyst samples show that the region around 3380 cm^{-1} and 1648 cm^{-1} are attributed to O-H bond stretching and bending vibrations of water, respectively. The infrared peak characteristics of P-O and V-O groups are observed in the region of 900-1200 cm^{-1}. An important band at 978 cm^{-1} which corresponds to symmetric stretching vibrations of V^{4+}=O group is found in VPO precursor sample. However this band is shifted to 948 cm^{-1} *via* calcined to activated VPO and Al-VPO samples, and this is ascribed to the stretching vibration of V^{5+}=O group [1]. It is interesting that the vibration band is broaden in the Ni-Al-VPO catalyst sample, and still appears weak stretching vibrations of V^{4+}=O and V^{5+}=O groups. The reason may be that the Ni component is incorporated into the framework of VPO and influences the structure of the VPO catalyst [2]. Besides, the band detected at 405-678 cm^{-1} can be assigned to the deformation vibrations of O-P-O groups of phosphate tetrahedral, the band at 1089 cm^{-1} can be due to asymmetric stretching of PO_4 groups and the band at 1164 cm^{-1} due to the antisymmetric stretching of PO_4 groups [3].

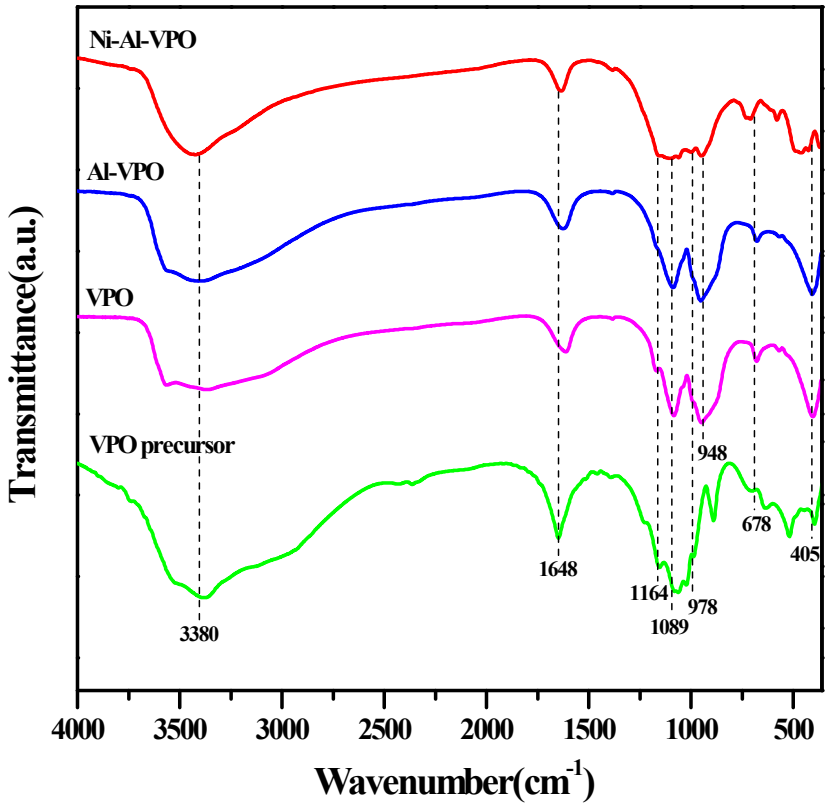

Figure S4

3.5 UV-vis spectra studies

In order to obtain the information of the vanadium oxidation state in VPO composite catalysts, the UV-vis diffuse reflectance spectra was carried out. From the literature it is clear that V^{5+} exhibits the charge transfer (CT) absorption band at around 400-500 nm whereas V^{4+} shows the charge transfer absorption band at around 220 nm [4]. In **Figure S5**, a broad band for VPO precursor was observed at 200-350 nm due to the charge transfer transition from O^{2-} to V^{4+} and another transition band from 660 nm due to d-d transition band of V^{4+} species [5]. In the case of the activated VPO and Al-VPO catalysts, the intensity of the d-d transition

band of V^{4+} become weak, and the broad band at 350-500 nm can be related to the charge transfer band of V^{5+} species. For the UV-vis spectra of Ni-Al-VPO catalyst, it is also found the broad band of V^{4+} and V^{5+} species. But the UV absorption wavelength occurs red shift phenomenon, the d-d transition band of V^{4+} and the charge transfer band of V^{5+} were changed to higher wavelength which at around 710nm and a band at 400-550 nm respectively. This indicates that doped Ni component influences the structure of the VPO. Additionally, the nickel phosphate showed a band at 314-370nm [6], which might be due to Ni (Ⅱ) cations interacting with the phosphate counter anions in the VPO framework, this result is well agreement with the XRD characterization.

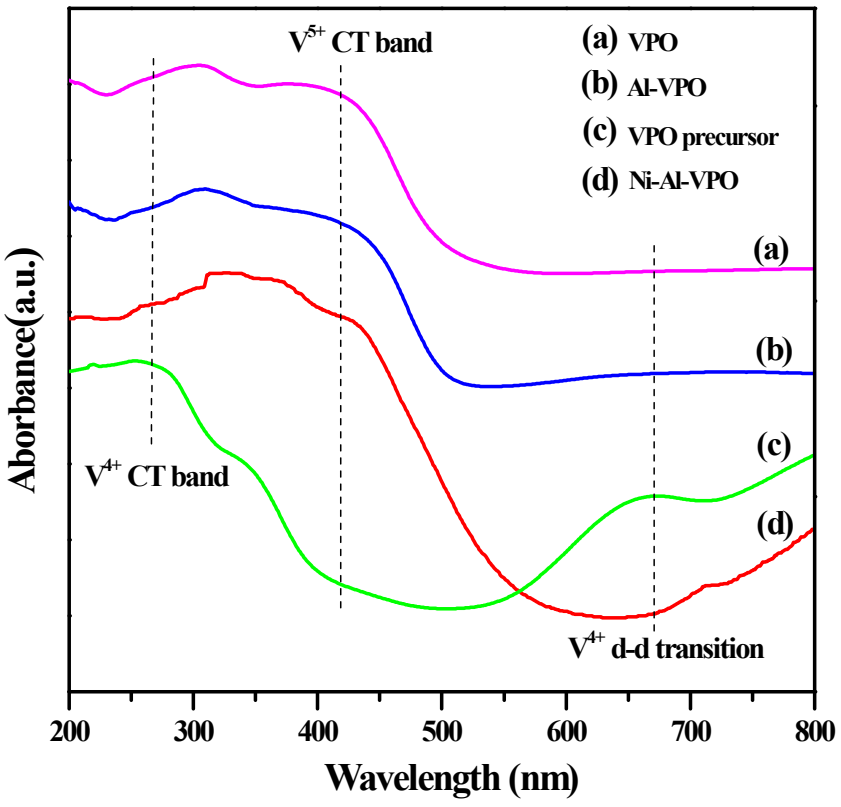

Figure S5

3.6 H_2 temperature-programmed reduction (H_2-TPR) studies

The reduction behaviors of the typical VPO composite catalysts were examined by the temperature programmed reduction (TPR), and the results are reported in **Figure S6**. The VPO precursor only shows a single reduction peak with maximum temperature at around 775 ^{o}C, attributable to the removal of oxygen atoms related to V^{4+} species [7]. The activated VPO and Al-VPO were found two reduction peaks, the main peaks at 616 ^{o}C and 644 ^{o}C were due to the removal of oxygen atoms associated with V^{5+} species [8], and the weak peaks at 720 ^{o}C and 759 ^{o}C were due to the removal of oxygen atoms associated with V^{4+} species. It is also found that the reduction peaks for Al-VPO catalyst were shifted to lower temperature compare to VPO sample, this implies that doped Al element of Al-VPO catalyst is easer to reduce than pure VPO. The similar phenomenon was occurred in the Ni-Al-VPO catalyst as well, the reduction peaks of V^{5+} group was shifted to much lower temperature at 596 ^{o}C. However, it is different that the reduction peak of V^{4+} to V^{3+} was became more prominent in the TPR of Ni-Al-VPO catalyst, in other words, the amounts of V^{4+} species was higher than V^{5+} species. Moreover, the first reduction peak at 495 ^{o}C can be assigned to the removal of oxygen atoms related to Ni^{2+} species in the $Ni_2P_2O_7$ phase [9], this suggests that the addition of Ni component leads to decease the reduction temperature of VPO catalyst. These results as well as the

characterizations of XRD and XPS indicate that the doped Ni component is not only has changed the structure of VPO but also enhanced the catalytic performance for the selective catalytic oxidation of cyclohexane.

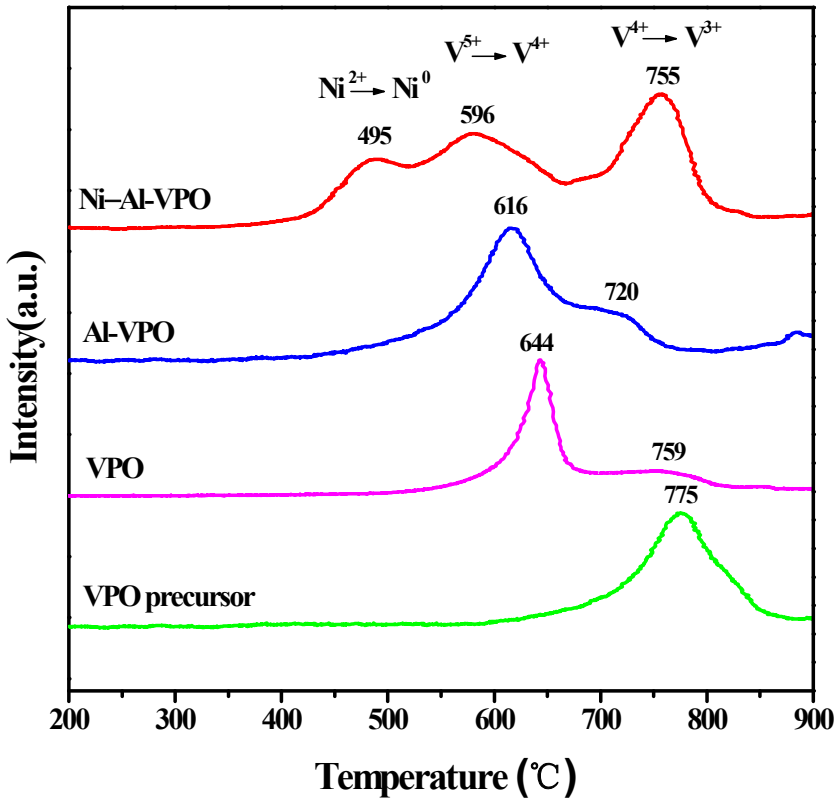

Figure S6

3.7 TEM studies

Transmission electron microscopy (TEM) characterization of typical VPO composite catalysts was shown in **Figure S7**. The TEM images of VPO precursor and Ni-Al-VPO composite catalyst showed monolithic particles, while the VPO and Al-VPO catalyst exhibited agglomerated irregular shaped platelets. In order to further obtain the insights on

interface of the catalyst and the crystal facet information (d-spacing) and size, the high-resolution transmission electron microscopy (**HRTEM**) images of samples were adopted, as shown in **Figure S7**. Obviously, two characteristic lattice fringes could be easily observed from the HRTEM images of Ni-Al-VPO sample. The fringes spacing of d=0.318 nm correspond to (204) lattice plane is assigned to $(VO)_2P_2O_7$, and the other fringes spacing of d=0.521 nm correspond to (101) lattice plane is assigned to β-$VOPO_4$. These studies confirm that the Ni-Al-VPO catalyst contain $(VO)_2P_2O_7$ phase and β-$VOPO_4$, which are good agreement with the XRD characterization. However, the HRTEM images of VPO precursor, VPO and Al-VPO samples showed no sign of lattice fringes; only amorphous speckle contrast is seen. The possible reason was that the three samples were very sensitive to the electron beam, and the aimed region of the sample was damaged by irradiated after a few seconds, which resulted in faint and diffuse lattice fringes. These results are consistent with literature reports by Kiely [10] and Hutchings [11, 12].

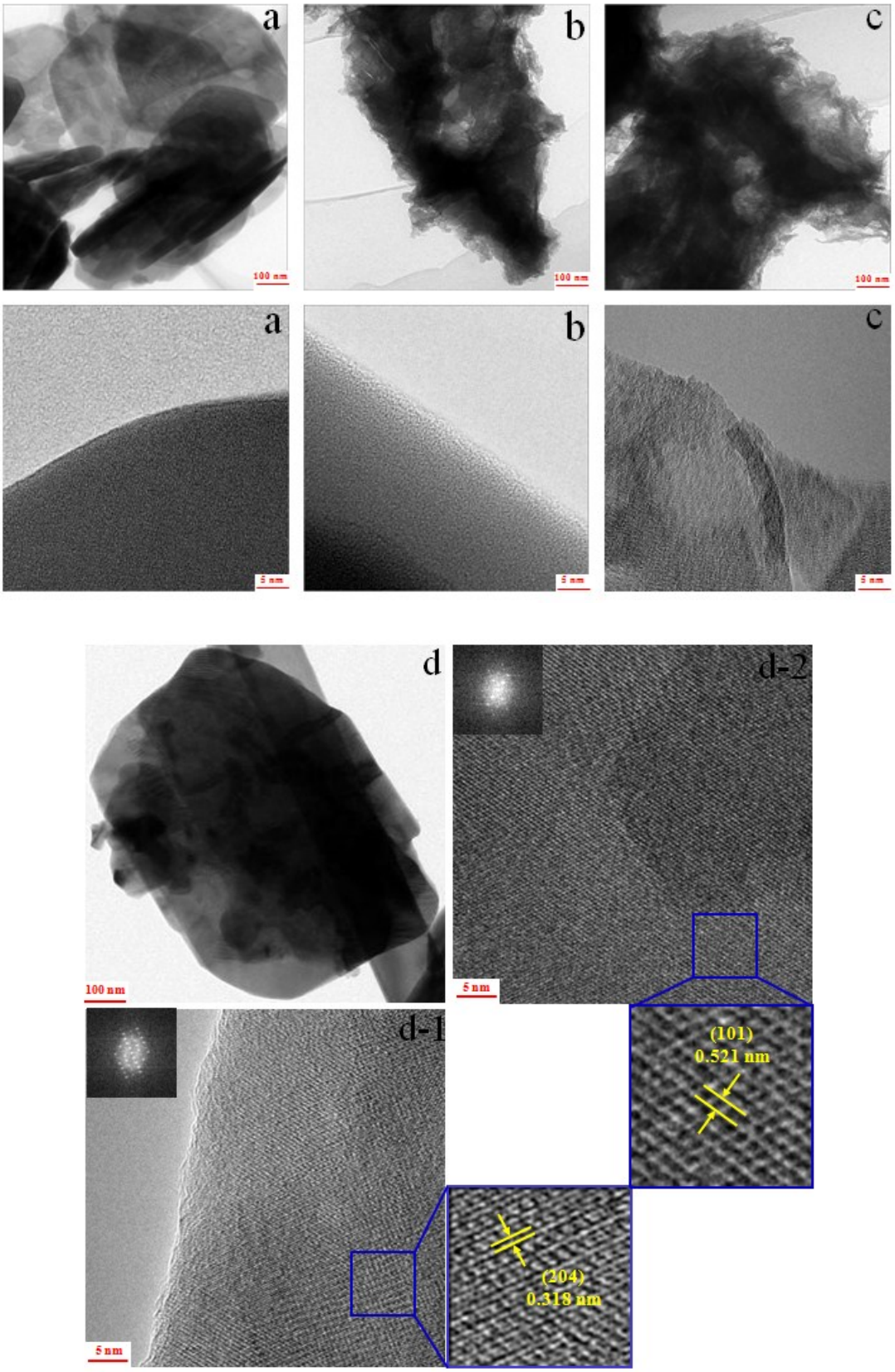
a
b
c
100 nm
100 nm
100 nm
a
b
c
5 nm
5 nm
5 nm
d
100 nm
d-2
5 nm
(101)
0.521 nm
d-1
5 nm
(204)
0.318 nm

Figure S7

References:

[1] G.C. Behera, K.M. Parida, *Appl. Catal. A: Gen.*, 2013 **464-465**, 364.

[2] V. Mahdavi, H.R. Hasheminasab, *J. Taiwan. Inst. Chem. E.*, 2015, **51**, 53.

[3] P. Borah, A. Datta, *Appl. Catal. A: Gen.*, 2010, **376**, 19.

[4] N.P. Rajan, G.S. Rao, V. Pavankumar, K.V.R. Chary, *Catal. Sci. Technol.*, 2014, **4**, 81.

[5] F. Cavani, S. Ligi, T. Monti, F. Pierelli, F. Trifirò, S. Albonetti, G Mazzoni, *Catal. Today*, 2000, **61**, 203.

[6] F. Wang, J.L. Dubois, W. Ueda, *Appl. Catal. A: Gen.*, 2010, **376**, 25.

[7] X.K. Li, W.J. Ji, J. Zhao, Z.B. Zhang, C.T. Au, *J. Catal*., 2006, **238**, 232.

[8] B.T. Pierini, E.A. Lombardo, *Mater. Chem. Phys.*, 2005, **92**, 197.

[9] Y. Takita, K. Sano, K. Kurosaki, N. Kawata, H. Nishiguchi, M. Ito, T. Ishihara, *Appl. Catal. A: Gen*., 1998, **167**, 49.

[10] C.J. Kiely, A. Burrows, S. Sajip, G.J. Hutchings, M.T. Sananes, A. Tuel, J.C. Volta, *J. Catal*., 1996, **162**, 31.

[11] J.A. Lopez-Sanchez, L. Griesel, J.K. Bartley, R.P. Wells, A. Liskowski, D. Su, R. Schlögl, J.C. Voltac, and G.J. Hutchings, *Phys. Chem. Chem. Phys.*, 2003, **5**, 3525.

[12] G.J. Hutchings, J.K. Bartley, J.M. Webster, J.A. Lopez-Sanchez, D.J. Gilbert, J.C. Kiely, A.F. Carley, S.M. Howdle, S. Sajip, S. Caldarelli, C. Rhodes, J.C. Volta, M. Poliakoff, *J. Catal*., 2001, **197**, 232.

3.8 The effects of molar ratio of cyclohexane to NO_2 on the oxidation reaction

The effects of molar ratio of cyclohexane to NO_2 on the oxidation reaction were studied. And the results (see **Table S1**) showed that the molar ratio of cyclohexane and NO_2 was also a significant factor to regulate the products selectivities from the oxidation of cyclohexane and NO_2. From the points of the selectivity of adipic acid, it is clearly found that the favorable molar ratio of cyclohexane with nitrogen dioxide is about 0.2:1 under the reaction time of 24 h and the reaction temperature of 80 ºC.

Table S1 Effect of molar ratio of cyclohexane with NO_2 on the oxidation reaction [a]

Molar ratio (cyclohexane:NO_2)	Conversion (%)	Selectivity (%)[b]				
		Adipic acid	Nitrocyclohexane	succinic acid	glutaric acid	cyclohexyl nitrate
1:1	18.2	62.9	19.3	3.2	0.7	9.9
0.8:1	20.6	63.7	18.5	3.5	1.6	9.8
0.6:1	23.5	68.2	17.6	3.7	1.3	7.2
0.4:1	29.5	72.9	17.2	4.0	1.2	3.6
0.2:1	40.4	78.2	14.8	4.3	1.3	0.2
0.1:1	48.1	66.4	13.1	7.5	11.5	0.2

[a] Reaction conditions: the reaction time is 24 h; reaction temperature: 80 ºC.

[b] the other products include cyclohexanol, cyclohexanone.

3.9 The elemental analysis of typical VPO composite catalysts

The elemental analysis using ICP-OES technique for the various VPO composite catalysts were shown in **Table S2**. For all of samples, the molar ratio of vanadium to phosphorous (V/P) is approximate to 1.2:1, which is consistent with the actual adding amount.

Table S2 Composition of the elements in the several VPO composite catalysts

Catalyst	Elements composition (wt%)				Molar ratio of P/V
	V	P	Al	Ni	
VPO precursor	27.8	19.8	-	-	1.17
VPO	28.6	20.5	-	-	1.18
Al-VPO	19.5	14.3	8.03	-	1.21
Ni-Al-VPO	17.1	12.3	7.88	14.4	1.18

3.10 Catalyst recycling and leaching on the oxidation reaction

In the present work, Ni-Al-VPO catalyst was easily separated and recovered from the solid phase products by filtration method, and the data of catalyst recycling and leaching in each reaction was summarized in **Table S3**. The results showed that the leaching of Ni-Al-VPO catalyst was ca 1.4% in each recycling process, and the total mass loss was ca 6.9% after five runs. The possible reason was that the small amount of Ni-Al-VPO composite catalyst was dissolved in nitric acid formed in the

oxidation reaction process, meanwhile, the physical loss of catalyst existed in the process of recycling.

Table S3 Data of Ni-Al-VPO catalyst recycling and leaching

Entry	Adding amount (g)	Recycling amount (g)	Leaching (%)
1	0.2011	0.1985	1.3
2	0.1985	0.1947	1.9
3	0.1947	0.1915	1.6
4	0.1915	0.1896	1.0
5	0.1896	0.1874	1.1
Average			1.4
Total			6.9